# Diversity Reception of DAPSK over Generalized Fading Channels

Yao Ma, *Member, IEEE*, Q. T. Zhang, *Senior Member, IEEE*, Robert Schober, *Member, IEEE*, and Subbarayan Pasupathy, *Fellow, IEEE*

To appear in the IEEE Transaction on Wireless Communications

**Abstract**

The accurate performance evaluation of differential amplitude and phase-shift keying (DAPSK) with post-detection equal gain combining (EGC) over generalized fading channels is of great theoretical interest and practical importance. In this paper, by using a decision variable-based moment generating function (DV-MGF) approach, exact error probability results for DAPSK over generalized Rician and Nakagami fading channels are derived, taking into account the effects of all the system and fading channel parameters. Several maximum-likelihood (ML) based detectors that do not require channel state information (CSI) are proposed for generalized Rician fading channels, and an exact bit error probability (BEP) union bound for the ML detection is derived. Assuming CSI a performance upper bound for DAPSK with EGC is also presented. Simulation and numerical results show when both detectors have no CSI, the conventional DAPSK detector may perform closely to (though worse than) the ML detector. However, the EGC receiver with CSI performs substantially better than the ML detector without CSI, and very closely to the coherent APSK detector.

**Index Terms**

Differential amplitude and phase-shift keying, Rician and Nakagami fading channels, maximum likelihood detection, fading correlation, decision variable, union bound, post-detection diversity

## I. Introduction

Differential amplitude and phase-shift keying (DAPSK) is an efficient modulation scheme that can be implemented in wireless communication systems without requiring channel state information (CSI) at the receiver side. For DAPSK modulation considered in this paper, the signal points lie on a few concentric

Yao Ma is with the Department of ECpE, Iowa State University, Ames, IA, 50011. Tel: 515-294-8382. Fax: 515-294-8432. E-mail: mayao@iastate.edu. Q. T. Zhang is with the Department of Electronic Engineering, City University of Hong Kong. Email: eekzhang@cityu.edu.hk. Robert Schober is with the Dept. of Electrical & Computer Engineering, University of British Columbia, 2356 Main Mall, Vancouver, BC, V6T 1Z4, Canada. E-mail: rschober@ece.ubc.ca. S. Pasupathy is with the Communications Group, Department of ECE, University of Toronto, 10 King's College Road, Toronto, Ontario, M5S 3G4, Canada. Fax: 1-416-978-4425. E-mail: pas@comm.utoronto.ca.

This paper has been presented in part at IEEE ICC'03, Anchorage, AL.

rings, with $N$ amplitude levels and $M$ phases [1], [2], and thus we use the notation DAPSK $(N, M)$, which may also be called $N$-DASK/$M$-DPSK [3], or star quadrature amplitude modulation (star-QAM) [4], [3], [5], [6]. In this scheme, both signal phases and amplitudes are modulated and differentially encoded. Due to its robustness to false phase locking and fading [4], and better error performance than DPSK [5], [6], DAPSK has attracted a lot of research interest in the last few years [4], [7], [8], [1], [2], [5], [6], [9], [3], [10], [11]. In [9], [12], DAPSK $(2, 8)$ [which is called 16-star QAM] with post-detection equal gain combining (EGC) over a Rayleigh fading channel with independent and identically distributed (i.i.d.) branches was studied. In [7], [8], some schemes for DAPSK combined with multi-carrier transmission were considered and the performances were evaluated by simulations for non-fading and frequency-selective Rayleigh fading channels. In [5], [6], the performance of DAPSK (2,8) over frequency-selective Rician fading channels with EGC assuming independent branches was analyzed.

However, the exact error probability of DAPSK with EGC over more realistic Rician fading channels (e.g. with correlated diversity branches due to the limitation of the receiver size) has not been investigated. Furthermore, to the authors' knowledge, an analytical result for the performance of DAPSK $(N, M)$ with EGC over Nakagami channels is not available in the literature, despite the versatility and usefulness of the Nakagami fading model in wireless communications [13].

In this paper, we derive the exact performance result for DAPSK $(N, M)$ with EGC over generalized Rician and Nakagami fading channels. We express the amplitude and phase decision variables (DVs) as quadratic forms, and derive the relevant moment generating function (MGF) expressions. By using the inverse Laplace transform (ILT) of the MGFs, the distributions of signal amplitude and phase are then expressed as single and double finite summations of some elementary functions, respectively. The new result is general and takes into account arbitrary diversity order, correlated signal branches with non-identical statistics, correlated noise, and non-zero Doppler fading bandwidth (e.g. fast fading).

In [1] several maximum-likelihood (ML) detectors based on two-symbol observations for Rayleigh fading channels with i.i.d branches were derived, and the results showed that the performance of the conventional DAPSK detector with EGC is very close to that of the ML detector. This motivates us to study this problem for generalized Rician fading channels. In this paper, several exact and approximate ML detectors for correlated and independent Rician fading diversity channels are proposed, and a new and exact bit error probability (BEP) union bound is derived.

With multiple symbol detection, or equivalently, after a less noisy reference signal is obtained, performance of DAPSK can be improved significantly [10], [11]. Therefore, it is of interest to obtain the performance of DAPSK when a perfect reference signal is available, that is, with CSI. Consequently, new performance results for DAPSK with CSI and EGC over general Rician and Nakagami fading channels are derived. Numerical and simulation results show that a properly designed conventional DAPSK detector (i.e. with an optimized ring ratio and proper decision boundaries) may achieve a BEP performance close to that of the

ML detector in general Rician channels. Also, the performance of DAPSK with CSI is significantly better than that without CSI.

The remainder of this paper is organized as follows. The signal model is introduced in Section II. Exact error probability formulas for amplitude and phase detection are presented in Sections III and IV, respectively. Several ML detectors for DAPSK signals over general Rician channels are proposed and a BEP union bound is derived in Section V. Further, the performance of DAPSK with CSI is derived in Section VI. We present some simulation and numerical results for DAPSK in Section VII. Finally, some conclusions are provided in Section VIII. Throughout this paper, we use superscripts $*$, T, H, $-1$ to represent the scalar conjugate, vector (or matrix) transpose, conjugate transpose, and matrix inversion, respectively. Re$(x)$ denotes the real part of the complex variable $x$, and $\det(\mathbf{A})$ is the determinant of matrix $\mathbf{A}$.

## II. Signal Model

We denote the signals received in the $i$th symbol interval over all $L$ diversity branches by the $L$-vector

$$\mathbf{x}(i) = \mathbf{c}(i)d(i) + \mathbf{n}(i), \tag{1}$$

where $d(i)$ is the differentially amplitude-and-phase encoded symbol. For DAPSK $(N, M)$, there are $N$ different amplitudes and $M$ different phase angles. $d(i) = \sqrt{\gamma}\beta^{a(i)}e^{j\theta(i)}$, where $a(i) \in \{0, 1, \ldots, N-1\}$ takes on $N$ possible values, and $\beta$ ($\beta > 1$) is the ring ratio. The scaling factor $\gamma$ is chosen to be $\gamma = [N(1-\beta^2)]/(1-\beta^{2N})$, so that the symbol energy is normalized to unity. $a(i) = a(i-1) + \Delta a(i) \mod N$, where $\Delta a(i) = a(i) - a(i-1)$ takes on $2N-1$ possible values $\{-N+1, \ldots, 0, \ldots, N-1\}$. The amplitude information is given by $\Delta a(i) \mod N$, which takes on $N$ possible values $\{0, 1, \ldots, N-1\}$. $\theta(i) \in \{2\pi m/M, m = 0, 1, \ldots, M-1\}$ is a DPSK modulated signal phase, and $j = \sqrt{-1}$. $b(i) = d(i)/d(i-1) = \beta^{\Delta a(i)}e^{j\Delta\theta(i)}$ is the data symbol carrying the amplitude and phase information, where $\Delta\theta(i) = \theta(i) - \theta(i-1)$ is the information phase. $\mathbf{c}(i) = [c_1(i), \ldots, c_L(i)]^{\top}$ is the $L \times 1$-size channel-coefficient vector. The noise vector $\mathbf{n}(i) = [n_1(i), \ldots, n_L(i)]^{\top}$, is a circularly symmetric zero-mean complex Gaussian process, with the average power $E[|n_k(i)|^2] = \sigma_k^2$ for $k = 1, \ldots, L$, where $E[\cdot]$ denotes expectation. We define the $L \times L$ noise correlation matrix as $\mathbf{R}_n(k) = \mathrm{E}\{\mathbf{n}(i)\mathbf{n}^{\mathrm{H}}(i-k)\}$, which takes into account the effect of both temporal and spatial noise correlation [14].

### A. Rician Fading Channels

We define the $L \times L$ channel spatio-temporal covariance matrix between the $L$ branches as $\mathbf{\Sigma}(n) = E\{(\mathbf{c}(i) - \boldsymbol{\mu}_c)(\mathbf{c}(i-n) - \boldsymbol{\mu}_c)^{\mathrm{H}}\}$, where $\boldsymbol{\mu}_c = E[\mathbf{c}(i)] = [\mu_{c,1}, \ldots, \mu_{c,L}]^{\top}$ is the line-of-sight (LOS) component of $(i)$. At the $l$th diversity branch, the signal power is defined as $\gamma_l = |c_l(i)|^2$, and the power of the diffuse component is $\tilde{\gamma}_l = |c_l(i) - \mu_{c,l}|^2$. The average of $\tilde{\gamma}_l$ is given by $\bar{\tilde{\gamma}}_l = E\{|c_l(i) - \mu_{c,l}|^2\} = [\mathbf{\Sigma}(0)]_{l,l}$, where

$[\mathbf{\Sigma}]_{l,l}$ denotes the $(l,l)$th diagonal element of the square matrix $\mathbf{\Sigma}$. The average signal power at the $l$th branch is then given by $\bar{\gamma}_l = \bar{\bar{\gamma}}_l + |\mu_{c,l}|^2 = (1+K_l)\bar{\bar{\gamma}}_l$, where $K_l = |\mu_{c,l}|^2/\bar{\bar{\gamma}}_l$ is the Rician factor.

For the $L$-fold diversity we define the signal power vector for all the branches as $\boldsymbol{\gamma} = [\gamma_1, \gamma_2, \ldots, \gamma_L]^\top$, and the diversity output power as $\gamma_{\text{tot}} = \sum_{l=1}^{L} \gamma_l$. For correlated branches, the MGF for $\gamma_{\text{tot}}$ is given by

$$\Phi_{\gamma_{\text{tot}}}(s) \;=\; E\left[\exp\left(\sum_{l=1}^{L}\gamma_l s\right)\right] = \exp(\boldsymbol{\mu}_c^{\text{H}}[\mathbf{I}_L/s - \mathbf{\Sigma}(0)]^{-1}\boldsymbol{\mu}_c)/\det(\mathbf{I}_L - s\mathbf{\Sigma}(0)),$$

where $\mathbf{I}_L$ is the $L \times L$ identity matrix. For independent branches, $\Phi_{\gamma_{\text{tot}}}(s)$ simplifies to [15]

$$\Phi_{\gamma_{\text{tot}}}(s) = \prod_{l=1}^{L} \frac{1+K_l}{1+K_l - s\bar{\gamma}_l} \exp\left(\frac{sK_l\bar{\gamma}_l}{1+K_l - s\bar{\gamma}_l}\right).$$

### *B. Nakagami Fading Channels*

For Nakagami channels, the instantaneous signal power at the $l$th branch, $\gamma_l = |c_l(i)|^2$, follows the gamma distribution with the probability density function (pdf) defined by [16] $f_{\gamma_l}(\gamma_l) = \frac{1}{\Gamma(m_l)}\left(\frac{m_l}{\bar{\gamma}_l}\right)^{m_l} \gamma_l^{m_l-1} e^{-\frac{m_l\gamma_l}{\bar{\gamma}_l}}$, where $\Gamma(m) = \int_0^\infty e^{-t}t^{m-1}dt$ is the Gamma function, $\bar{\gamma}_l = E[|c_l(i)|^2]$ is the average signal power at the $l$th branch, and $m_l \geq 0.5$ is the fading parameter. For $L$-fold diversity with independent diversity branches, the MGF for $\gamma_{\text{tot}}$ is

$$\Phi_{\gamma_{\text{tot}}}(s) = \prod_{l=1}^{L}(1 - s\bar{\gamma}_l/m_l)^{-m_l}. \tag{2}$$

For the correlated fading case, assuming that the fading figure $m$ is identical for the different branches, we get the MGF of the total signal power as [17]

$$\Phi_{\gamma_{\text{tot}}}(s) = \det(\mathbf{I}_L - s\mathbf{M}/m)^{-m}, \tag{3}$$

where $\mathbf{M}$ is the fading covariance matrix, which can be computed from the power covariance matrix $\mathbf{R}_\gamma = E[\boldsymbol{\gamma}\boldsymbol{\gamma}^T] - E[\boldsymbol{\gamma}]E[\boldsymbol{\gamma}]^T$ (e.g. see [18]).

### *C. Conventional Differential Detection with EGC Diversity*

For conventional differential detection, the reference signal is given by the received signal in the previous symbol interval $\mathbf{x}(i-1)$, and thus the complex decision variable (DV) for the signal phase is given by [9], [19]

$$D_p = \mathbf{x}^{\text{H}}(i-1)\mathbf{x}(i) = \sum_{l=1}^{L} x_l^*(i-1)x_l(i). \tag{4}$$

The phase decision for symbol $b(i) = d(i)/d(i-1)$ is given by[1] $\Delta\hat{\theta}(i) = 2\pi\hat{m}/M$, where $\hat{m} = \text{argmax}_m\, \text{Re}\{D_p e^{-j2\pi m/M}\}$, or equivalently, $\hat{m} = \text{argmin}_m\, |\Delta\theta_p - 2\pi m/M|$, where $\Delta\theta_p$ is the phase of

[1]The $m$ used here should be distinguished from the Nakagami $m$ parameter.

$D_p$ before the hard decision.

For amplitude detection the amplitude comparison at the $l$th branch is based on the ratio $R_l = |x_l(i)|/|x_l(i-1)|$. Ideally, $R_l$ takes on $2N-1$ possible values, $\beta^{-N+1}, \ldots, \beta^{N-1}$, cf. Figure 1. Let the decision boundaries be given by $\{B_n\}$ for $n = -N+1, \ldots, 0, 1, \ldots, N$, where $B_{-N+1} = 0$ and $B_N = \infty$, and $B_{n-1} < \beta^{n-1} < B_n < \beta^n$ holds. When $B_n < R_l < B_{n+1}$, the corresponding decision rule is that $\Delta\hat{a}(i) = n$ if $n \geq 0$, and $\Delta\hat{a}(i) = n + N$ if $n < 0$. When we combine the multi-channel received signal by post-detection EGC, the DV is defined as [9]

$$D_a = [\mathbf{x}^{\mathrm{H}}(i)\mathbf{x}(i)]/[\mathbf{x}^{\mathrm{H}}(i-1)\mathbf{x}(i-1)] = \frac{\sum_{l=1}^{L}|x_l(i)|^2}{\sum_{l=1}^{L}|x_l(i-1)|^2}. \tag{5}$$

Since post-detection EGC for the amplitude detection corresponds to square-law combining, we replace the original decision boundaries by $\{[B_n]^2\}_{n=-N+1}^{N}$.

The average BEP for DAPSK $(N, M)$ is given by [1], [5]

$$\bar{P}_b = \frac{1}{\log_2(NM)}[\log_2(N)\bar{P}_{a,b} + \log_2(M)\bar{P}_{p,b}], \tag{6}$$

where $\bar{P}_{a,b}$ and $\bar{P}_{p,b}$ are the average BEPs for the amplitude and phase detection, respectively. Assuming that the error probabilities of the phase and amplitude detection are independent, the average symbol error probability (SEP) is given by

$$\bar{P}_s = 1 - (1 - \bar{P}_{a,s})(1 - \bar{P}_{p,s}) = \bar{P}_{a,s} + \bar{P}_{p,s} - \bar{P}_{a,s}\bar{P}_{p,s}, \tag{7}$$

where $\bar{P}_{a,s}$ and $\bar{P}_{p,s}$ are the average SEPs for the amplitude and phase detection, respectively.

## III. Performance of Amplitude Detection

We derive new results for the exact error probability of DAPSK $(N, M)$ for arbitrary Rician and Nakagami fading channels. The average amplitude SEP and BEP equal

$$\bar{P}_{a,s} = 1/N^2 \sum_{n_1=0}^{N-1}\sum_{n_2=0}^{N-1} P_{a,s}(n_1, n_2) \quad \text{and} \quad \bar{P}_{a,b} = 1/N^2 \sum_{n_1=0}^{N-1}\sum_{n_2=0}^{N-1} P_{a,b}(n_1, n_2),$$

where $P_{a,s}(n_1, n_2)$ and $P_{a,b}(n_1, n_2)$ are, respectively, the conditional SEP and BEP of amplitude detection assuming signals with amplitudes $\sqrt{\gamma}\beta^{n_1}$ and $\sqrt{\gamma}\beta^{n_2}$ are transmitted in the $(i-1)$th and $i$th symbol intervals, respectively. Let $\Delta n = n_2 - n_1$, and due to the cyclic differential amplitude encoding, we obtain

$$P_{a,s}(n_1, n_2) = \begin{cases} 1 - \Pr(B_{\Delta n}^2 < D_a < B_{\Delta n+1}^2) & \Delta n = 0 \\ 1 - \Pr(B_{\Delta n}^2 < D_a < B_{\Delta n+1}^2) - \Pr(B_{\Delta n-N}^2 < D_a < B_{\Delta n-N+1}^2) & \Delta n > 0 \\ 1 - \Pr(B_{\Delta n}^2 < D_a < B_{\Delta n+1}^2) - \Pr(B_{\Delta n+N}^2 < D_a < B_{\Delta n+N+1}^2) & \Delta n < 0 \end{cases} \tag{8}$$

where $\Pr(A)$ denotes the probability that event A occurs. For the BEP calculation $P_{a,b}(n_1, n_2) = 1/\log_2(N)$ $\sum_{\Delta\hat{n}=-N+1}^{N-1} w_a(\Delta\hat{n}, \Delta n) \Pr(B_{\Delta\hat{n}-1}^2 < D_a < B_{\Delta\hat{n}}^2)$, where $w_a(\Delta\hat{n}, \Delta n)$ is a weighting factor (Hamming

distance) depending on the amplitude symbol-bit mapping scheme. When the phases and amplitudes are independently Gray-coded, for $N = 2$ and 4, $w_a(\Delta\hat{n}, \Delta n)$ is a function of $\Delta\hat{\hat{n}} = (\Delta\hat{n} - \Delta n) \mod N$. For $N = 2$, $w_a(\Delta\hat{n}, \Delta n) = \begin{cases} 0 & \Delta\hat{\hat{n}} = 0 \\ 1 & \Delta\hat{\hat{n}} = 1 \end{cases}$. For $N = 4$, $w_a(\Delta\hat{n}, \Delta n)$ is listed in Table I[2]. Also, for high SNR we can show that $P_{a,b}(n_1, n_2) \simeq \frac{1}{\log_2 N} P_{a,s}(n_1, n_2)$ for $n_1, n_2 \in \{0, 1, \ldots, N-1\}$.

Since $\Pr(B^2_{\Delta n} < D_a < B^2_{\Delta n+1}) = \Pr(D_a < B^2_{\Delta n+1}) - \Pr(D_a < B^2_{\Delta n})$, we only have to evaluate a probability of the form $\Pr(D_a < B^2_{\Delta n})$, and all the other terms can be computed in the same manner. Obviously, $\Pr(D_a < B^2_{\Delta n}) = \Pr(-B^2_{\Delta n} \sum_{l=1}^{L} |x_l(i-1)|^2 + \sum_{l=1}^{L} |x_l(i)|^2 < 0)$, which can be expressed as the probability that a quadratic form is smaller than zero. Specifically, $\Pr(D_a < B^2_{\Delta n}) = \Pr(\tilde{D}_a < 0)$, where $\tilde{D}_a = \mathbf{v}^{\mathrm{H}}\mathbf{Q}\mathbf{v} < 0$, $\mathbf{v} = [\mathbf{x}^\top(i-1), \mathbf{x}^\top(i)]^\top$, and

$$\mathbf{Q} = \begin{bmatrix} -B^2_{\Delta n}\mathbf{I}_L & \mathbf{0}_{L\times L} \\ \mathbf{0}_{L\times L} & \mathbf{I}_L \end{bmatrix},$$

where $\mathbf{0}_{L\times L}$ denotes the $L \times L$ zero matrix. We first derive the MGF for the DV $\tilde{D}_a$ for Rician and Nakagami fading channels, and then present a Gauss-Chebyshev quadrature (GCQ) formula [20] to compute $\Pr(\tilde{D}_a < 0)$.

### *A. Rician Fading Channels*

As in (1), let $d(i-1) = \sqrt{\gamma}\beta^{n_1} e^{j2m_1\pi/M}$ and $d(i) = \sqrt{\gamma}\beta^{n_2} e^{j2m_2\pi/M}$ denote the signals in the $(i-1)$th and $i$th symbol intervals, respectively. Also we let $b(i) = d(i)/d(i-1) = \beta^{\Delta a(i)} e^{j\Delta\theta(i)} = \beta^{\Delta n} e^{j2\Delta m\pi/M}$ denote the ratio of the signals in two adjacent symbol intervals, where $\Delta n = n_2 - n_1$ and $\Delta m = m_2 - m_1$. Conditioned on $n_1, n_2, \Delta n$, and $\Delta m$, the covariance matrix and the mean of $\mathbf{v}$, are respectively given by

$$\mathbf{P}_v = \begin{bmatrix} \mathbf{\Sigma}(0)\gamma\beta^{2n_1} + \mathbf{R}_n(0) & \mathbf{\Sigma}^{\mathrm{H}}(1)\gamma\beta^{2n_1+\Delta n} e^{-j2\Delta m\pi/M} + \mathbf{R}_n^{\mathrm{H}}(1) \\ \mathbf{\Sigma}(1)\gamma\beta^{2n_1+\Delta n} e^{j2\Delta m\pi/M} + \mathbf{R}_n(1) & \mathbf{\Sigma}(0)\gamma\beta^{2n_2} + \mathbf{R}_n(0) \end{bmatrix} \tag{9}$$

$$\boldsymbol{\mu}_v = [\boldsymbol{\mu}_c^\top\sqrt{\gamma}\beta^{n_1}, \boldsymbol{\mu}_c^\top\sqrt{\gamma}\beta^{n_1+\Delta n} e^{j2\Delta m\pi/M}]^\top e^{j2m_1\pi/M}. \tag{10}$$

Employing a result for the distribution of a non-central Gaussian quadratic form [21], [22], the MGF for $\tilde{D}_a$ is given by

$$\Phi_{\tilde{D}_a}(s) = \frac{\exp(\boldsymbol{\mu}_v^{\mathrm{H}}[\mathbf{Q}^{-1}s^{-1} - \mathbf{P}_v]^{-1}\boldsymbol{\mu}_v)}{\det(\mathbf{I}_{2L} - s\mathbf{P}_v\mathbf{Q})}, \tag{11}$$

where the factor of $e^{j2m_1\pi/M}$ in (10) no longer exists indicating its irrelevance to the BEP evaluation. When $\mathbf{R}_n(1) = \mathbf{0}_{L\times L}$, i.e., temporally white noise, $\Phi_{\tilde{D}_a}(s)$ is identical for different $\Delta\theta(i)$, and thus without loss of generality we can assume $\Delta\theta(i) = 0$ (that is $\Delta m = 0$).

[2]Note that for $N > 4$, $w_a(\Delta\hat{n}, \Delta n)$ is in general a function of both $\Delta\hat{n}$ and $\Delta n$.

### B. Nakagami Fading Channels

We derive the MGF for $\tilde{D}_a$ over correlated Nakagami fading channels. We assume a slow Nakagami fading channel, namely $\mathbf{c}(i) = \mathbf{c}(i-1) = \mathbf{c}$. We also assume spatially and temporally white noise, and thus without loss of generality we assume $\Delta\theta(i) = 0$ below.

For convenience, we rewrite $\tilde{D}_a = \sum_{l=1}^{L} \tilde{D}_{a,l}$, where $\tilde{D}_{a,l} = \mathbf{v}_l^{\mathrm{H}} \mathbf{q} \mathbf{v}_l$ is the amplitude DV at the $l$th branch, $\mathbf{v}_l = [c_l\sqrt{\gamma}\beta^{n_1} + n_l(i-1), c_l\sqrt{\gamma}\beta^{n_2} + n_l(i)]^\top$, and $\mathbf{q} = \begin{bmatrix} -B_{\Delta n}^2 & 0 \\ 0 & 1 \end{bmatrix}$. Let $\mathbf{z}_l = c_l\mathbf{e}$, where $\mathbf{e} = [\sqrt{\gamma}\beta^{n_1}, \sqrt{\gamma}\beta^{n_2}]^\top$. Conditioned on $\mathbf{z}_l$, $\mathbf{v}_l$ has a Gaussian distribution with mean $\mathbf{z}_l$ and co-variance $\mathbf{P}_{n,l}$, where $\mathbf{P}_{n,l}$ is the correlation matrix for the noise vector $[n_l(i-1), n_l(i)]^\top$, given by

$$\mathbf{P}_{n,l} = \begin{bmatrix} \sigma_l^2 & \rho_{n,l}^* \sigma_l^2 \\ \rho_{n,l}\sigma_l^2 & \sigma_l^2 \end{bmatrix}.$$

Here, $\sigma_l^2$ and $\rho_{n,l} = E(n_l(i)n_l^*(i-1))/\sigma_l^2$ represent, respectively, the noise power and the noise temporal correlation coefficient at the $l$th branch, for $l = 1, \ldots, L$. The conditional MGF for $\tilde{D}_{a,l}$ at the $l$th branch is obtained as $\Phi_l(s|c_l) = E[\exp[s\mathbf{v}_l^{\mathrm{H}}\mathbf{q}\mathbf{v}_l]] = \exp\left(s|c_l|^2 g_l\right)/\det(\mathbf{I}_2 - s\mathbf{q}\mathbf{P}_{n,l})$, where $g_l = \mathbf{e}^\top[(s\mathbf{q})^{-1} - \mathbf{P}_{n,l}]^{-1}\mathbf{e}$.

Conditioned on $\mathbf{c}$, $\mathbf{v}_l^{\mathrm{H}}\mathbf{q}\mathbf{v}_l$ (for $l = 1, \ldots, L$) are mutually independent variables, and therefore

$$\Phi(s|\mathbf{c}) \;=\; \prod_{l=1}^{L} \Phi_l(s|c_l) = \frac{\exp\left(s\sum_{l=1}^{L}|c_l|^2 g_l\right)}{\prod_{l=1}^{L}\det(\mathbf{I}_2 - s\mathbf{q}\mathbf{P}_{n,l})}. \tag{12}$$

Next, we shall average $\Phi(s|\mathbf{c})$ over the distribution of $\mathbf{c}$ [23], [18]. By using (3), the average MGF for the amplitude DV $\tilde{D}_a$ over correlated Nakagami channels is given by

$$\Phi_{\tilde{D}_a}(s) = \frac{\det(\mathbf{I}_L - s\mathrm{diag}[g_1, \ldots, g_L]\mathbf{M}/m)^{-m}}{\prod_{l=1}^{L}\det(\mathbf{I}_2 - s\mathbf{q}\mathbf{P}_{n,l})}, \tag{13}$$

where $\mathrm{diag}[g_1, \ldots, g_L]$ is a diagonal matrix that is formed by setting elements $g_1, \ldots, g_L$ on its main diagonal. Similarly, by using (2), the MGF for $\tilde{D}_a$ over Nakagami channels with independent but non-identically distributed (i.n.d.) branches can be obtained as

$$\Phi_{\tilde{D}_a}(s) = \frac{\prod_{l=1}^{L}(1 - sg_l\bar{\gamma}_l/m_l)^{-m_l}}{\prod_{l=1}^{L}\det(\mathbf{I}_2 - s\mathbf{q}\mathbf{P}_{n,l})}. \tag{14}$$

### C. Cumulative Distribution Function (CDF) of the Amplitude DV

Once the MGF expressions for $\tilde{D}_a$ over general Rician and Nakagami fading channels are derived, the cdf $\Pr(\tilde{D}_a < 0)$ can be evaluated by the inverse Laplace integral,

$$\Pr(\tilde{D}_a < 0) = \frac{1}{2\pi}\mathrm{Re}\left(\int_{c-j\infty}^{c+j\infty} \frac{\Phi_{\tilde{D}_a}(-s)}{js} ds\right), \tag{15}$$

where $c$ is a small real constant in the convergence region. Let $s = s_0 + j\omega$ and $\omega = s_0 \tan(\phi/2)$, where $s_0$ is the saddle point of $\frac{\Phi_{\tilde{D}_a}(-s)}{s}$, which can be computed recursively by Newton's method [24]. Equation (15) can be evaluated by a GCQ formula [20],

$$\Pr(\tilde{D}_a < 0) \quad = \quad \frac{1}{2\hat{N}} \sum_{n=1}^{\hat{N}} \hat{\Phi}\left(\frac{(2n-1)}{2\hat{N}}\pi\right) + \hat{R}_{\hat{N}}, \tag{16}$$

where $\hat{\Phi}(\theta) = \Phi_{\tilde{D}_a}(-s_0 - js_0\tan(\theta/2))(1 - j\tan(\theta/2))$, and $\hat{R}_{\hat{N}}$ is a residual term which vanishes for $\hat{N} \to \infty$. Finally, we note that the amplitude error probability result proposed in this section, when specialized to the DAPSK (2,8) and the independent Rayleigh fading case, is equivalent to those given in [9], [12]. However, our result is applicable to more general fading channels, and to DAPSK $(N, M)$ with different $N$'s and $M$'s.

## IV. Performance of Phase Detection

The phase detection error probability can be determined by the joint distribution of the real part $D_R$ and imaginary part $D_I$ of the DV $D_p$ at the receiver output given by (4), as shown by

$$D_R = \frac{1}{2}(D_p + D_p^*) = \mathbf{v}^{\mathrm{H}}\mathbf{Q}_R\mathbf{v} \quad \text{and} \quad D_I = -\frac{1}{2}j(D_p - D_p^*) = \mathbf{v}^{\mathrm{H}}\mathbf{Q}_I\mathbf{v},$$

where $\mathbf{Q}_R = \begin{bmatrix} \mathbf{0}_{L\times L} & 0.5\mathbf{I}_L \\ 0.5\mathbf{I}_L & \mathbf{0}_{L\times L} \end{bmatrix}$, $\mathbf{Q}_I = \begin{bmatrix} \mathbf{0}_{L\times L} & -0.5j\mathbf{I}_L \\ 0.5j\mathbf{I}_L & \mathbf{0}_{L\times L} \end{bmatrix}$, and $\mathbf{v} = [\mathbf{x}^\top(i-1), \mathbf{x}^\top(i)]^\top$. The phase of $D_p$ is denoted by $\Delta\theta_p$, and we define its cdf as $F(\theta) = \Pr(-\pi/2 < \Delta\theta_p \le \theta)$. Note that since $\mathbf{v}$ is a function of the transmitted signal amplitudes $\sqrt{\gamma}\beta^{n_1}$ and $\sqrt{\gamma}\beta^{n_2}$, and so are $D_R$ and $D_I$. For convenience, we define

$$x_R = D_R = \mathbf{v}^{\mathrm{H}}\mathbf{Q}_R\mathbf{v} \quad \text{and} \quad x_I(\theta) = D_I - \tan(\theta)D_R = \mathbf{v}^{\mathrm{H}}[\mathbf{Q}_I - \tan(\theta)\mathbf{Q}_R]\mathbf{v},$$

which allows us to express the phase cdf as [25]

$$F(\theta) = \begin{cases} \Pr(x_R > 0, x_I(\theta) \le 0) & \theta \in [-\pi/2, \pi/2) \\ \Pr(x_R > 0) + \Pr(x_R < 0, x_I(\theta) > 0) & \theta \in [\pi/2, 3\pi/2) \end{cases}. \tag{17}$$

To evaluate $F(\theta)$, we define the joint MGF for $x_R$ and $x_I(\theta)$ as

$$\Phi(s_1, s_2) = E[\exp(s_1 x_R + s_2 x_I(\theta))] = E[\exp(\mathbf{v}^{\mathrm{H}}\mathbf{Q}(s_1, s_2)\mathbf{v})], \tag{18}$$

where $\mathbf{Q}(s_1, s_2) = s_1\mathbf{Q}_R + s_2[\mathbf{Q}_I - \tan(\theta)\mathbf{Q}_R]$. For Rician fading channels, the joint MGF is thus

$$\Phi(s_1, s_2) = \frac{\exp(\boldsymbol{\mu}_v^{\mathrm{H}}\mathbf{F}(s_1, s_2)\boldsymbol{\mu}_v)}{\det(\mathbf{I}_{2L} - \mathbf{Q}(s_1, s_2)\mathbf{P}_v)}, \tag{19}$$

where $\mathbf{F}(s_1, s_2) = ([\mathbf{Q}(s_1, s_2)]^{-1} - \mathbf{P}_v)^{-1}$, and $\mathbf{P}_v$ and $\boldsymbol{\mu}_v$ are given by (9) and (10), respectively.

For Nakagami fading channels, with the assumption that $\Delta\theta(i) = e^{j2\Delta m\pi}$, the complex variable $\mathbf{v}^{\mathrm{H}}\mathbf{Q}(s_1,s_2)\mathbf{v}$ can be rewritten as $\mathbf{v}^{\mathrm{H}}\mathbf{Q}(s_1,s_2)\mathbf{v} = \sum_{l=1}^{L}\mathbf{v}_l^{\mathrm{H}}\mathbf{q}(s_1,s_2)\mathbf{v}_l$, where $\mathbf{v}_l = [c_l\sqrt{\gamma}\beta^{n_1}e^{j2m_1\pi} + n_l(i-1), c_l\sqrt{\gamma}\beta^{n_2}e^{j2(m_1+\Delta m)\pi} + n_l(i)]^{\top}$, and $\mathbf{q}(s_1,s_2) = 0.5\begin{bmatrix} 0 & s_1 - s_2[j+\tan(\theta)] \\ s_1 + s_2[j-\tan(\theta)] & 0 \end{bmatrix}$.

Assuming spatially uncorrelated noise and using a procedure similar to that for obtaining the MGF for the amplitude detection, we can derive the joint MGF expression for the phase detection DVs in correlated Nakagami channels as[3]

$$\Phi(s_1,s_2) = \frac{\det(\mathbf{I}_L - \mathrm{diag}[g_1(s_1,s_2),\ldots,g_L(s_1,s_2)]\mathbf{M}/m)^{-m}}{\prod_{l=1}^{L}\det(\mathbf{I}_2 - \mathbf{q}(s_1,s_2)\mathbf{P}_{n,l})}, \tag{20}$$

where $g_l(s_1,s_2) = \mathbf{e}^{\top}[[\mathbf{q}(s_1,s_2)]^{-1} - \mathbf{P}_{n,l}]^{-1}\mathbf{e}$, and $\mathbf{e} = [\sqrt{\gamma}\beta^{n_1}, \sqrt{\gamma}\beta^{n_2}e^{j2\Delta m\pi}]^{\top}$. Similarly, by using (2), the joint MGF for i.n.d Nakagami diversity channels can be obtained as

$$\Phi_{\tilde{D}_p}(s) = \frac{\prod_{l=1}^{L}(1 - g_l(s_1,s_2)\bar{\gamma}_l/m_l)^{-m_l}}{\prod_{l=1}^{L}\det(\mathbf{I}_2 - s\mathbf{q}(s_1,s_2)\mathbf{P}_{n,l})}. \tag{21}$$

Next, the joint cdf for $\Pr(x_R, x_I(\theta))$ can be evaluated by a GCQ formula as

$$\begin{aligned}\Pr(x_R>0, x_I(\theta)>0) &= \frac{1}{8N_1N_2}\sum_{n_1=1}^{N_1}\sum_{n_2=1}^{N_2}\left[\tilde{\Phi}\left(\frac{(2n_1-1)\pi}{2N_1}, \frac{(2n_2-1)\pi}{2N_2}\right)\right. \\ &\quad \left. + \tilde{\Phi}\left(\frac{(2n_1-1)\pi}{2N_1}, -\frac{(2n_2-1)\pi}{2N_2}\right)\right] + \tilde{R}_{N_1,N_2},\end{aligned} \tag{22}$$

where $\tilde{\Phi}(\theta_1,\theta_2) = \Phi[c_1 + jc_1\tan(\theta_1/2), c_2 + jc_2\tan(\theta_2/2)][1 - j\tan(\theta_1/2)][1 - j\tan(\theta_2/2)]$, $\tilde{R}_{N_1,N_2}$ is a remainder term which vanishes as $N_1$ and $N_2$ increase, and $c_1$ and $c_2$ are the saddle points of $\Phi(s_1,s_2)$ with respect to $s_1$ and $s_2$, respectively. The numerical search for $c_1$ and $c_2$ can be implemented by the 2-D Newton's method as discussed in [25].

Then the correct symbol decision probability can be expressed in terms of $F(\theta)$ given in (17), as shown by $P_{s,M}^{c}(\alpha_m|n_1,n_2) = F(\alpha_m + \pi/M|n_1,n_2) - F(\alpha_m - \pi/M|n_1,n_2)$, where $\alpha_m = 2\pi\Delta m/M$ is the transmitted information phase. Thus, the conditional SEP is given by $P_{s,M}(\alpha_m|n_1,n_2) = 1 - P_{s,M}^{c}(\alpha_m|n_1,n_2)$, and the average SEP for phase detection is equal to

$$\bar{P}_{s,M} = \frac{1}{MN^2}\sum_{m=1}^{M}\sum_{n_1=1}^{N}\sum_{n_2=1}^{N}P_{s,M}(\alpha_m|n_1,n_2). \tag{23}$$

The exact BEP expression for phase detection applicable to arbitrary bit-mapping schemes is

$$\bar{P}_{b,M} = \frac{(MN)^{-2}}{\log_2 M}\sum_{\Delta\hat{m}\neq\Delta m}\sum_{n_1,n_2} w_p(\Delta m, \Delta\hat{m})[F(2\pi(\Delta\hat{\hat{m}} + 0.5)/M) - F(2\pi(\Delta\hat{\hat{m}} - 0.5)/M)], \tag{24}$$

where $\Delta\hat{\hat{m}} = (\Delta\hat{m} - \Delta m) \mod M$, and $w_p(\Delta m, \Delta\hat{m})$ is the weighting factor determined by the phase

[3]When the noise in all the branches is also temporally uncorrelated, the MGF is identical for different $\Delta\theta(i)$, thus we can assume $\Delta m = 0$ without loss of generality. However, for the temporally correlated noise, we have to average the result over all $\{\Delta m\}$.

bit-mapping scheme. For example, for Gray-coded $M$-phase signalling with $M = 8$ and 16, $w_p(\Delta m, \Delta\hat{m})$ can be obtained using the results in [26], [15], [25]. Assuming Gray-coding, by using (24) the exact BEP expressions for $M = 8$ and 16 are, respectively, given by [15], [25]

$$\bar{P}_{b,8} = 2/3(1 - [F(3\pi/8) - F(-\pi/8)]), \tag{25}$$

$$\bar{P}_{b,16} = \frac{1}{2}\left[F\left(\frac{17}{16}\pi\right) - F\left(\frac{1}{16}\pi\right) + F\left(\frac{15}{16}\pi\right) + F\left(\frac{13}{16}\pi\right) - F\left(\frac{9}{16}\pi\right) - F\left(\frac{3}{16}\pi\right)\right], \tag{26}$$

where, again, the dependence of $F(\theta)$ on $n_1$ and $n_2$ has been suppressed for the sake of brevity. Certainly, (25) and (26) have to be averaged over $n_1$ and $n_2$. After having derived the performance of the DAPSK EGC receiver without CSI, we consider some maximum-likelihood (ML) detection schemes for Rician channels (without CSI) based on two-symbol observations, which provide a performance upper bound for non-coherent detection of DAPSK.

## V. Maximum Likelihood Detection for Rician Channels

### A. Generalized Rician Fading Channels

We derive the maximum-likelihood (ML) detector for DAPSK signals over general Rician fading channels. The task is to find the ML estimate of $b(i)$ based on the observation of vector $\mathbf{v} = [\mathbf{x}^\top(i-1), \mathbf{x}^\top(i)]^\top$, where $\mathbf{x}(i)$ is defined in (1). The log-likelihood function for $\mathbf{v}$ over general Rician fading channels is given by

$$\ln f_{\mathbf{v}}(\mathbf{v}) = -(\mathbf{v} - \boldsymbol{\mu}_v)^{\text{H}}\mathbf{P}_v^{-1}(\mathbf{v} - \boldsymbol{\mu}_v) - \ln[\det(\pi^L\mathbf{P}_v)], \tag{27}$$

where $\mathbf{P}_v$ and $\boldsymbol{\mu}_v$ are given by (9) and (10), respectively. The ML estimate for $b(i)$ is given by

$$\hat{b}(i) = \underset{b(i)}{\operatorname{argmin}}\{\min_{d(i-1)}\{J_1(d(i-1), b(i))\}\}, \tag{28}$$

where $J_1(d(i-1), b(i))$ is the decision metric given by

$$J_1(d(i-1), b(i)) = (\mathbf{v} - \boldsymbol{\mu}_v)^{\text{H}}\mathbf{P}_v^{-1}(\mathbf{v} - \boldsymbol{\mu}_v) + \ln[\det(\mathbf{P}_v)]. \tag{29}$$

We refer to the detector based on (28) as the ideal ML detector. The optimization in (28) requires the calculation of matrix product and the inversion of the $2L \times 2L$ matrix $\mathbf{P}_v$, and thus entails a complexity of $O(L^3)$. Further, (28) requires minimization with respect to both $d(i-1)$ and $b(i)$, and thus it entails a total complexity of $O(N^2M^2L^3)$.

### B. Independent Rician Channels

In the case of independent diversity branches and white noise, $\boldsymbol{\Sigma}(0)$ and $\boldsymbol{\Sigma}(1)$ are both diagonal matrices, and also $\mathbf{R}_n(0) = \sigma_n^2\mathbf{I}_L$, and $\mathbf{R}_n(1) = \mathbf{0}_{L\times L}$. The decision metric $J_1(d(i-1), b(i))$ can be simplified

considerably. The joint pdf of $\mathbf{v}$ conditioned on $d(i-1)$ and $b(i)$ can be expressed as

$$f_{\mathbf{v}}(\mathbf{v}|d(i-1),b(i)) = \prod_{l=1}^{L} f_{x_l(i)}[x_l(i)|x_l(i-1),d(i-1),b(i)]f_{x_l(i-1)}[x_l(i-1)|d(i-1)], \quad (30)$$

where we used the fact that $f_{x_l(i)}[x_l(i-1)|d(i-1),b(i)] = f_{x_l(i-1)}[x_l(i-1)|d(i-1)]$. Also in (30),

$$f_{x_l(i)}[x_l(i)|x_l(i-1),d(i-1),b(i)] = \frac{1}{\pi\omega_{2,l}}\exp\left(-\frac{|x_l(i)-\omega_{1,l}|^2}{\omega_{2,l}}\right), \quad (31)$$

$$f_{x_l(i-1)}[x_l(i-1)|d(i-1)] = \frac{1}{\pi\omega_{3,l}}\exp\left(-\frac{|x_l(i-1)-\mu_{c,l}d(i-1)|^2}{\omega_{3,l}}\right). \quad (32)$$

In (31) and (32), for the $l$th branch the parameters $\omega_{1,l},\omega_{2,l}$, and $\omega_{3,l}$ are, respectively, given by

$$\omega_{1,l} = \mu_{c,l}d(i) + \frac{\rho_{t,l}\gamma_{f,l}|d(i-1)|^2 b(i)[x_l(i-1)-\mu_{c,l}d(i-1)]}{(1+\gamma_{f,l}|d(i-1)|^2)},$$

$$\omega_{2,l} = \sigma_n^2\left[\frac{1+\gamma_{f,l}(1+|b(i)|^2)|d(i-1)|^2+(1-\rho_{t,l}^2)|\gamma_{f,l}|^2|d(i-1)|^4|b(i)|^2}{1+\gamma_{f,l}|d(i-1)|^2}\right],$$

$$\omega_{3,l} = [1+\gamma_{f,l}|d(i-1)|^2]\sigma_n^2,$$

where $\rho_{t,l} = E[(c_l(i)-\mu_{c,l})(c_l(i-1)-\mu_{c,l})^*]/[\mathbf{\Sigma}(0)]_{l,l}$ is the temporal fading correlation coefficient at the $l$th branch. Also, $\gamma_{f,l} = [\mathbf{\Sigma}(0)]_{l,l}/\sigma_n^2$ is the average SNR for the diffuse fading component.

Thus, we can get a new decision metric as

$$J_2(d(i-1),b(i)) = \sum_{l=1}^{L}\left[\frac{|x_l(i)-\omega_{1,l}|^2}{\omega_{2,l}} + \frac{|x_l(i-1)-\mu_{c,l}d(i-1)|^2}{\omega_{3,l}} + \ln(\omega_{2,l}\omega_{3,l})\right]. \quad (33)$$

The ML estimate for $b(i)$ can be obtained by using an operation similar to that used in (28) by replacing $J_1(d(i-1),b(i))$ with $J_2(d(i-1),b(i))$. We refer to the ML detector based on $J_2(d(i-1),b(i))$ as the simplified ML (SML) detector in this paper. The equivalence of the ML and the SML detectors in independent Rician fading channels is verified by our simulations. However, the SML detector still involves a multi-dimensional minimization with a complexity of $O(N^2M^2L)$. We note that for Rayleigh fading channels, (i.e. $\boldsymbol{\mu}_c = \mathbf{0}_{L\times 1}$), the decision metric $J_2(d(i-1),b(i))$ reduces to that presented in [1], if we re-define the noise power to $\sigma_n^2 = 1$. For Rayleigh fading channels, the phase of $d(i-1)$ is not required for the decision metric, and the minimization of $J_2(d(i-1),b(i))$ involves a complexity of $O(NM^2L)$.

### *C. Asymptotic ML detector*

To further simplify the decision metrics for independent Rician fading channels, as in [1], we assume high SNR ($\gamma_{f,l} \gg 1$) and small Doppler bandwidth ($\rho_{t,l} \simeq 1$). Thus, we get

$$\omega_{1,l} \simeq \mu_{c,l}b(i)d(i-1) + b(i)[x_l(i-1)-\mu_{c,l}d(i-1)] = b(i)x_l(i-1), \quad (34)$$

$$\omega_{2,1} \simeq \sigma_n^2\left(1+|b(i)|^2\right). \quad (35)$$

Also, in (33) the second term $\frac{|x_l(i-1)-\mu_{c,l}d(i-1)|^2}{\omega_{3,l}}$ is a function of $d(i-1)$, but is independent of $b(i)$. Since only $b(i)$ is the desired data symbol, the second term in (33) can be dropped.

With these approximations, the metric in (33) is simplified to

$$J_3(b(i)) = \sum_{l=1}^{L} \left[ \frac{|x_l(i) - b(i)x_l(i-1)|^2}{\sigma_n^2 \left(1 + |b(i)|^2\right)} + \ln\left(1 + |b(i)|^2\right) \right]. \tag{36}$$

Obviously, $J_3(b(i))$ is independent of $d(i-1)$. Let us re-write $J_3(b(i))$ as $J_3(\Delta n, \Delta m)$, where $b(i) = \beta^{\Delta n} e^{2j\Delta m\pi/M}$, then the phase and amplitude decisions are given by

$$\{\Delta\hat{n}, \Delta\hat{m}\} \;=\; \underset{\Delta n, \Delta m}{\operatorname{argmin}} \{J_3(\Delta n, \Delta m)\}. \tag{37}$$

We call the resulting detector the asymptotic ML (AML) detector. We note that in (36) only the knowledge of the ring ratio $\beta$ and the average noise power $\sigma_n^2$ is required.[4] The implementation of (37) involves a complexity of $O(NML)$. Actually (37) can be further simplified, because the phase decision for $\Delta m$ in (37) is independent of the amplitude decision, and can be expressed as [5]

$$\Delta\hat{m} = \underset{m}{\operatorname{argmax}}\, \mathrm{Re}\{D_p e^{-j2\pi m/M}\}, \tag{38}$$

where $D_p$ is given by (4). Obviously the phase decision for the AML detector is equivalent to that of the conventional EGC receiver. This result demonstrates that the product EGC detector for phase decision is asymptotically optimum (for high SNR and slow fading) in independent Rician fading channels. Next, the amplitude decision is given by $\Delta\hat{n} = \operatorname{argmin}_{\Delta n}\{J_3(\Delta n, \Delta\hat{m})\}$, where $\Delta\hat{m}$ is the decision output of (38). The complexity of the resulting AML detector is $O((N+M)L)$ for DAPSK $(N, M)$.

### *D. BEP Union Bound*

The BEP union upper bound is the weighted summation of the pair-wise error probability (PEP) associated with the amplitude and phase detection. For clarity of the presentation, some symbols are defined below. For the decision metric defined in (28), let $b(i) = \beta^{\Delta n} e^{j2\pi\Delta m/M}$, $d(i-1) = \sqrt{\gamma}\beta^{n_1} e^{j2\pi m_1/M}$, and $d(i) = \sqrt{\gamma}\beta^{n_1+\Delta n} e^{j2\pi(m_1+\Delta m)/M}$, which correspond to the transmitted symbols. Also, in case a pair-wise error event, we define $\hat{b}(i) = \beta^{\Delta\hat{n}} e^{j2\pi\Delta\hat{m}/M}$, $\hat{d}(i-1) = \sqrt{\gamma}\beta^{\hat{n}_1} e^{j2\pi\hat{m}_1/M}$, and $\hat{d}(i) = \sqrt{\gamma}\beta^{\hat{n}_1+\Delta\hat{n}} e^{j2\pi(\hat{m}_1+\Delta\hat{m})/M}$, which correspond to the symbol decisions (which may be erroneous) selected by the ML detector.

We note that in [1], a BEP union bound for the AML detector in an i.i.d Rayleigh fading channel was given, but a bound for the ideal ML detector has not been derived. In [2], a union bound for disjoint amplitude and phase detection of DAPSK with maximum ratio combining (MRC) and weighted MRC (WMRC) schemes

[4] We point out for the Rayleigh fading decision metric shown in (9) of [1] to be valid, the received signal must be re-scaled first by a factor of $1/\sigma_n$, so that the resulting noise variance is unity. Thus, the knowledge of the average noise power is also required for implementation of (9) in [1].

[5] We note that this simplification has not been pointed out in [1] for DAPSK signal.

was derived. These methods, however, are not applicable to the ideal ML detector in Rician fading channels. For the ML detector given in (28) for generalized Rician fading, we propose to calculate the BEP union bound as

$$P_u = \frac{(NM)^{-2}}{\log_2(NM)} \sum_{d(i-1),b(i)} \sum_{\hat{d}(i-1)} \sum_{\substack{\hat{b}(i) \\ \hat{b}(i)\neq b(i)}} [w_p(\Delta m, \Delta\hat{m}) + w_a(\Delta n, \Delta\hat{n})] P_2[b(i) \to \hat{b}(i)|d(i-1), b(i)] \tag{39}$$

where $\Delta n, \Delta\hat{n}$, $\Delta m$, and $\Delta\hat{m}$ are the amplitude and phase changes determined by $b(i)$ and $\hat{b}(i)$, and $w_a(\Delta n, \Delta\hat{n})$ and $w_p(\Delta m, \Delta\hat{m})$ are the weighting factors discussed in Sections III and IV, respectively. In (39), $P_2[b(i) \to \hat{b}(i)|d(i-1), b(i)]$ is the PEP that conditioned on $d(i-1)$ the transmitted signal $b(i)$ is detected as $\hat{b}(i)$.

When the noise is white we can use the symmetry property of the signal phases and simplify the double summation $\sum_{d(i-1),b(i)}$, and (39) can be reduced to

$$P_u = \frac{N^{-2}}{\log_2(NM)} \sum_{n_1,\Delta n} \sum_{\hat{d}(i-1)} \sum_{\hat{b}(i)\neq b(i)} [w_p(\Delta m, \Delta\hat{m}) + w_a(\Delta n, \Delta\hat{n})] P_2[b(i) \to \hat{b}(i)|d(i-1), b(i)]. \tag{40}$$

Next, we show how to evaluate the PEP $P_2[b(i) \to \hat{b}(i)|d(i-1), b(i)]$, which completes the evaluation of the BEP union bound. It is obvious that $P_2[b(i) \to \hat{b}(i)|d(i-1), b(i)] = \Pr\{D(d(i-1), b(i), \hat{d}(i-1), \hat{b}(i)) < 0\}$, where $D(d(i-1), b(i), \hat{d}(i-1), \hat{b}(i)) = J_1(\hat{d}(i-1), \hat{b}(i)) - J_1(d(i-1), b(i))$ is the DV, and we suppress the argument of $D$ below for conciseness. In the DV, $J_1(d(i-1), b(i)) = (\mathbf{v}-\boldsymbol{\mu}_v)^{\mathrm{H}}\mathbf{P}_v^{-1}(\mathbf{v}-\boldsymbol{\mu}_v) + \ln[\det(\mathbf{P}_v)]$ is defined in (29), and $J_1(\hat{d}(i-1), \hat{b}(i)) = (\mathbf{v}-\hat{\boldsymbol{\mu}}_v)^{\mathrm{H}}\hat{\mathbf{P}}_v^{-1}(\mathbf{v}-\hat{\boldsymbol{\mu}}_v) + \ln[\det(\hat{\mathbf{P}}_v)]$, where $\hat{\boldsymbol{\mu}}_v = \begin{bmatrix} \boldsymbol{\mu}_c\hat{d}(i-1) \\ \boldsymbol{\mu}_c\hat{d}(i) \end{bmatrix}$, and $\hat{\mathbf{P}}_v = \begin{bmatrix} \boldsymbol{\Sigma}(0)\gamma\beta^{2\hat{n}_1} + \mathbf{R}_n(0) & \boldsymbol{\Sigma}^{\mathrm{H}}(1)\gamma\beta^{2\hat{n}_1+\Delta\hat{n}}e^{-j2\Delta\hat{m}\pi/M} + \mathbf{R}_n^{\mathrm{H}}(1) \\ \boldsymbol{\Sigma}(1)\gamma\beta^{2\hat{n}_1+\Delta\hat{n}}e^{j2\Delta\hat{m}\pi/M} + \mathbf{R}_n(1) & \boldsymbol{\Sigma}(0)\gamma\beta^{2\hat{n}_2} + \mathbf{R}_n(0) \end{bmatrix}$.

Using the fact that $J_1(\hat{d}(i-1), \hat{b}(i)) = [(\mathbf{v}-\boldsymbol{\mu}_v) + (\boldsymbol{\mu}_v - \hat{\boldsymbol{\mu}}_v)]^{\mathrm{H}}\hat{\mathbf{P}}_v^{-1}[(\mathbf{v}-\boldsymbol{\mu}_v) + (\boldsymbol{\mu}_v - \hat{\boldsymbol{\mu}}_v)] + \ln[\det(\hat{\mathbf{P}}_v)]$, and after some manipulations, we can express the DV $D$ as a quadratic form plus a constant term as $D = \mathbf{w}^{\mathrm{H}}\tilde{\mathbf{Q}}\mathbf{w} + a$, where $a = \ln[\det(\hat{\mathbf{P}}_v)] - \ln[\det(\mathbf{P}_v)]$, $\mathbf{w} = \begin{bmatrix} \mathbf{v}-\boldsymbol{\mu}_v \\ \boldsymbol{\mu}_v - \hat{\boldsymbol{\mu}}_v \end{bmatrix}$, and $\tilde{\mathbf{Q}} = \begin{bmatrix} \hat{\mathbf{P}}_v^{-1} - \mathbf{P}_v^{-1} & \hat{\mathbf{P}}_v^{-1} \\ \hat{\mathbf{P}}_v^{-1} & \hat{\mathbf{P}}_v^{-1} \end{bmatrix}$. To compute the PEP $\Pr(D<0)$, we need to evaluate the MGF for $D$, which is

$$\Phi_D(s) = \frac{\exp(\bar{\mathbf{w}}^{\mathrm{H}}[\tilde{\mathbf{Q}}^{-1}s^{-1} - \mathbf{P}_w]^{-1}\bar{\mathbf{w}} + sa)}{\det(\mathbf{I}_{4L} - s\mathbf{P}_w\tilde{\mathbf{Q}})}, \tag{41}$$

where $\bar{\mathbf{w}}$ is the mean of $\mathbf{w}$ and is given by $\bar{\mathbf{w}} = \begin{bmatrix} \mathbf{0}_{2L\times 1} \\ \boldsymbol{\mu}_v - \hat{\boldsymbol{\mu}}_v \end{bmatrix}$. Further, $\mathbf{P}_w$ is the covariance matrix of $\mathbf{w}$ and $\mathbf{P}_w = \begin{bmatrix} \mathbf{P}_v & \mathbf{0}_{2L\times 2L} \\ \mathbf{0}_{2L\times 2L} & \mathbf{0}_{2L\times 2L} \end{bmatrix}$, where $\mathbf{P}_v$ is defined in (9). The PEP can be computed by using (15) and (16) and replacing $\Phi_{\tilde{D}_a}(s)$ with $\Phi_D(s)$ given in (41).

By using (41) and (39) [or (40)], the exact BEP union bound for the ML detector over generalized Rician fading channels can be evaluated. We note that the PEP evaluation method proposed above is general and can be used to evaluate the exact BEP union bound for many other detectors in generalized Rician fading, e.g. the AML detector proposed in Section V-C, and the MRC and WMRC detectors proposed in [2]. However, the derivation procedure is omitted here due to space limitations. For the union bound calculation in (39) all combinations of $\hat{d}(i-1)$ have to be taken into account, which is computationally quite expensive. If we assume the knowledge of $d(i-1)$, which may be obtained by using decision feedback (e.g. see [10], [11]), the computation in (28) can be reduced greatly by removing the minimization with respect to $d(i-1)$. With the knowledge of $d(i-1)$, the union bound in (39) is reduced to

$$P_u = \frac{(NM)^{-2}}{\log_2(NM)} \sum_{d(i-1),b(i)} \sum_{\hat{b}(i)\neq b(i)} [w_p(\Delta m, \Delta\hat{m}) + w_a(\Delta n, \Delta\hat{n})] P_2[b(i) \to \hat{b}(i) | d(i-1), b(i)], \tag{42}$$

where in the PEP expression $P_2[b(i) \to \hat{b}(i)|d(i-1), b(i)]$ we need to change $J_1(\hat{d}(i-1), \hat{b}(i))$ to $J_1(d(i-1), \hat{b}(i))$ and modify $\hat{\boldsymbol{\mu}}_v$ and $\hat{\mathbf{P}}_v$ accordingly.

Our simulation results given later show that the ML detector performs better than the EGC receiver, especially in Rician fading with a high $K$ factor. However, the ML detector requires accurate knowledge of the channel statistics, and is computationally very expensive to implement. It is thus interesting to know how much the performance of the DAPSK EGC receiver can be improved if CSI is available. This topic is studied next.

## VI. Performance of DAPSK with CSI

We derive the error probability of the DAPSK EGC receiver assuming CSI, which gives a performance upper bound for DAPSK with decision feedback (DF) channel estimation and detection [10], [11] [6]. In the ideal case, instead of $\mathbf{x}(i-1)$, the reference signal is given by $\mathbf{x}_{\text{ref}}(i) = \mathbf{c}(i)\hat{d}(i-1)$, and we assume $\hat{d}(i-1) = d(i-1)$[7]. For Rician fading channels, assuming $\Delta\theta(i) = 0$, (9) is replaced by

$$\mathbf{P}_v = \begin{bmatrix} \boldsymbol{\Sigma}(0)\gamma\beta^{2n_1} & \boldsymbol{\Sigma}(0)\gamma\beta^{n_1+n_2} \\ \boldsymbol{\Sigma}(0)\gamma\beta^{n_1+n_2} & \boldsymbol{\Sigma}(0)\gamma\beta^{2n_2} + \mathbf{R}_n(0) \end{bmatrix}, \tag{43}$$

and $\boldsymbol{\mu}_v = [\boldsymbol{\mu}_c^{\top}\sqrt{\gamma}\beta^{n_1}, \boldsymbol{\mu}_c^{\top}\sqrt{\gamma}\beta^{n_2}]^{\top}$. For Nakagami fading channels, the amplitude DV is $\tilde{D}_a = \sum_{l=1}^{L} \mathbf{v}_l^{\text{H}}\mathbf{q}\mathbf{v}_l$, where $\mathbf{v}_l = [c_l\sqrt{\gamma}\beta^{n_1}, c_l\sqrt{\gamma}\beta^{n_2} + n_l(i)]^{\top}$, and $\mathbf{q} = \begin{bmatrix} -B_{\Delta n}^2 & 0 \\ 0 & 1 \end{bmatrix}$. For correlated diversity branches, the

[6] In [27], the performance for APSK (2,8) (named as 16-star QAM therein) with coherent detection is studied. Note that the data decision in [27] is based on polygonal decision boundaries in the two-dimensional signal plane, and is different from the coherent detection of DAPSK studied in this section.

[7] Note that the effect of error propagation of the decision feedback symbols can be studied by using a Markov-chain steady-state analysis, as shown in [28]. However, that is beyond of the scope of this paper.

MGFs for the amplitude and phase detection are, respectively,

$$\Phi_{\tilde{D}_a}(s) = \frac{\det(\mathbf{I}_L - s\text{diag}[g_1,\ldots,g_L]\mathbf{M}/m)^{-m}}{\prod_{l=1}^{L}\det(\mathbf{I}_2 - s\mathbf{q}\mathbf{P}'_{n,l})} \tag{44}$$

$$\text{and} \quad \Phi(s_1,s_2) = \frac{\det(\mathbf{I}_L - \text{diag}[g_1(s_1,s_2),\ldots,g_L(s_1,s_2)]\mathbf{M}/m)^{-m}}{\prod_{l=1}^{L}\det(\mathbf{I}_2 - \mathbf{q}(s_1,s_2)\mathbf{P}'_{n,l})}, \tag{45}$$

where $\mathbf{P}'_{n,l}$ is the correlation matrix for the vector $[0, n_l(i)]^\top$, given by $\mathbf{P}'_{n,l} = \begin{bmatrix} 0 & 0 \\ 0 & \sigma_l^2 \end{bmatrix}$. The result for the i.n.d branches can be obtained by replacing $\mathbf{P}_{n,l}$ with $\mathbf{P}'_{n,l}$ in (14) and (21), respectively. By substituting the results above into (11), (13), (19), and (20), the coherent detection (CD) error probability $P_{\text{CD}}$ for the DAPSK EGC receiver with CSI over general Rician and Nakagami fading channels can be evaluated.

## VII. Simulation and Numerical Results

Some performance results for the DAPSK EGC receiver with and without CSI, and the ML detector in fading channels are presented in this section.

### *A. Rician Fading Channels*

An equal correlation model is assumed for the Rician fading case, e.g., $\mathbf{\Sigma}(0) = \begin{bmatrix} 1 & \rho_c & \rho_c \\ \rho_c & 1 & \rho_c \\ \rho_c & \rho_c & 1 \end{bmatrix}$ for $L = 3$. When $\rho_c = 0$, we have an independent fading channel model. With the assumptions that the fading rates in different diversity branches are identical (i.e. $B_{f,l} = B_f$, $l = 1,\ldots,L$, where $B_{f,l}$ is the fading bandwidth at the $l$th branch), and that the spatial and temporal correlations can be separated, we set $\mathbf{\Sigma}(1) = \rho_t\mathbf{\Sigma}(0)$, where $\rho_t$ is the temporal fading correlation coefficient. We assume Clark's fading spectrum, that is, $\rho_t = J_0(2\pi B_f T)$, where $J_0(x)$ is the zeroth order Bessel function of the first kind, $T$ is a symbol period. The Rician factor $K$ is assumed to be identical for all branches, and the LOS component vector $\boldsymbol{\mu}_c$ is assumed to be co-phased, i.e. all the elements of $\boldsymbol{\mu}_c$ have the identical phases. Nevertheless, it should be noted (see [29]) that the performance loss due to the spatial fading correlation would be less severe if $\boldsymbol{\mu}_c$ was not co-phased. We also assume the noise is spatially and temporally white. As in [1], we set $B_n = \beta^{n-0.5}$ for $n = -N+1,\ldots,N-1$, and our extensive numerical computations (not shown here) suggest that this boundary setting is also near optimum for DAPSK with EGC in a large range of different parameters for Rician and Nakagami fading channels. First, we present some simulation results for DAPSK $(2,8)$ with independent-branch dual-diversity ($L = 2$) over a Rician fading channel with $B_f T = 0.02$ in Fig. 2 (for $K = 5$ dB) and Fig. 3 (for $K = 10$ dB), respectively. For the ML detector we use (28) with $J_1(d(i-1), b(i))$ or (33). To reduce the simulation complexity we assume $d(i-1)$ is known to the receiver (which may be obtained by using decision feedback of previous output symbols), and the minimization is with respect to

(w.r.t.) $b(i)$ only. The simulation results in Figs. 2 and 3 confirm the accuracy of our analytical results for the conventional EGC detector with and without CSI. Also, the BEP union bound [computed by using eq. (42)] for the ML detector becomes tighter when the average SNR increases and when the Rician $K$-factor becomes larger (e.g 10 dB). The SNR gap between the EGC detector and the ML detector (both without CSI) tends to increase for a larger $K$ factor. On the other hand, the BEP of the EGC receiver with coherent detection (CD) is substantially lower than that of the ML detector, e.g. around 1.9 dB improvement around a BEP level of $10^{-3}$ for $K = 5$ dB.

Next, we present numerical results for the BEP performance of the DAPSK EGC receiver with different ring ratios $(1.1 - 3.0)$ for independent and correlated Rician fading channels. DAPSK $(2, 8)$ and DAPSK $(4, 16)$ are considered in Figs. 4 and 5, respectively. The results show that the optimum ring ratio (yielding the lowest BEP) for DAPSK (2,8) lies within the range of (1.8,2.2), and that for DAPSK (4,16) lies within (1.4, 1.6), i.e., DAPSK (4,16) requires a smaller ring ratio than that of DAPSK (2,8). This is because the BEP of DAPSK is in general influenced more by the innermost ring than the outer rings. For a given ring ratio the radius of the innermost ring decreases when the number of rings $N$ becomes larger. Therefore, the optimum ring ratio for DAPSK(4,16) should be smaller than that for DAPSK(2,8), to avoid the excessive loss of SNR in the innermost ring. The results also show that the BEP performance of DAPSK (4,16) exhibits a larger variation than that of DAPSK (2,8) when $\beta$ changes, i.e., DAPSK (4,16) is more sensitive to $\beta$ than DAPSK (2,8). This observation can be explained by the fact that DAPSK (4,16) has four possible amplitude levels, and given the same symbol energy, its signal space decision regions are much smaller than those of DAPSK (2,8), and thus its performance is more sensitive to the ring ratio. When the average SNR increases, the optimum ring ratio tends to increase slightly. Therefore, for the following we set $\beta = 2$ for DAPSK (2,8) and $\beta = 1.4$ for DAPSK (4,16).

The BEPs of DAPSK with conventional detection and CD, and that of square-QAM with CD (all with EGC) are presented in Fig. 6 for $L = 3$ independent diversity branches. As expected, DAPSK with higher level modulation (4,16) results in a poorer performance than with $(2, 8)$. The performance of DAPSK (2,8) with CD is close to that of 16-QAM. However, DAPSK $(4, 16)$ performs quite poorly even with perfect CSI.

### *B. Nakagami Fading Channels*

Let us consider an uniform linear antenna array (with $L = 3$) operating in a slow Nakagami fading channel (where $B_f T = 0$). In particular, we consider a correlated channel with normalized power covariance matrix [18] $\mathbf{R}_\gamma = \begin{bmatrix} 1 & 0.795 & 0.605 \\ 0.795 & 1 & 0.795 \\ 0.605 & 0.795 & 1 \end{bmatrix}$, and an i.i.d. channel with $\mathbf{R}_\gamma = \mathbf{I}_L$. In Figs. 7 and 8, an independent Nakagami fading channel with $m = 0.7$ and $L = 3$ is assumed. We show the influence of the ring ratio $\beta$ on the phase, amplitude, and average BEPs of the DAPSK EGC receiver in Fig. 7 for an SNR of 24 dB.

It is observed that for both DAPSK (2,8) and (4,16), the phase detection BEP decreases monotonically as $\beta$ increases within the interval $[1.1, 3]$. This phenomenon can be explained by the fact that as the ring ratio $\beta$ increases, for a fixed SNR the smallest signal amplitude (signal points in the innermost rings) decreases, which dominates the phase BEP performance. However, the amplitude detection BEP has a more intricate relationship with $\beta$. For DAPSK (2,8) the amplitude BEP decreases monotonically as $\beta$ increases; but for DAPSK (4,16), the amplitude BEP has a minimum around $\beta = 1.6$. In fact, as $\beta$ increases, the amplitude ratio decision regions increase which tends to improve the performance; but the smallest signal amplitude decreases, which tends to degrade the performance. This tradeoff causes the phenomenon observed for DAPSK $(4, 16)$. Next, we study the optimum $\beta$ for the DAPSK EGC receiver in Fig. 8. The result shows that as the SNR increases, the BEP becomes more sensitive to $\beta$. Also, $\beta = 1.8$ (for DAPSK (2,8)) and $\beta = 1.3$ (for DAPSK (4,16)) give optimum performance for $m = 0.7$. (For results not shown here, we also observe that as $m$ increases, the optimum $\beta$ tends to increase, e.g. when $m = 2.5$, $\beta = 2$ seems to be optimum for DAPSK (2,8).)

Finally, we study the effect of correlated branches on the SEPs of DAPSK (2,8), APSK (2,8) (studied in [27]), and 16 square-QAM in a Nakagami channel with $m = 2.5$ in Fig. 9. The result shows that the performance of DAPSK (2,8) with CD is only slightly worse than that of APSK (2,8) at small SNRs, and is almost identical to that of the latter for high SNRs. Both of them suffer an SNR loss of about 1.5 dB w.r.t. 16-QAM for both independent and correlated fading at high SNRs, and show an SNR improvement of about 2.5 dB w.r.t. the conventional detection of DAPSK.

## VIII. Conclusions

In this paper, exact error probability formulas for DAPSK $(N, M)$ over generalized Rician and Nakagami fading channels were derived, taking into account the effects of different system and fading channel parameters. Results on the effects of the different ring ratios, decision boundaries, and channel parameters on the performance of the DAPSK EGC receiver have been presented. In comparison, the DAPSK (2,8) constellation is significantly more efficient than DAPSK $(4, 16)$ in the BEP sense. The conventional DAPSK EGC detector may perform closely to (though worse than) the ML detector when both detectors have no CSI. However, the EGC detector with CD (i.e. CSI) gives substantially better performance than the ML detector without CSI, and performs very closely to the coherent APSK detector.

## References

[1] C.-D. Chung, "Differentially amplitude and phase-encoded QAM for the correlated Rayleigh-fading channel with diversity reception," *IEEE Trans. Commun.*, vol. 45, pp. 309–321, March 1997.

[2] J. Y. Lee, Y. M. Chung, and S. U. Lee, "Postdetection diversity receiver for DAPSK signals on the Rayleigh- and Rician-fading channel," *IEEE Trans. Veh. Technol.*, vol. 50, pp. 1193–1202, Sep. 2001.

[3] N. A. B. Svensson, "On differentially encoded star 16QAM with differential detection and diversity," *IEEE Trans. Veh. Technol.*, vol. 44, pp. 586–593, Aug. 1995.

[4] W. T. Webb, L. Hanzo, and R. Steele, "Bandwidth efficient QAM schemes for Rayleigh fading channels," *IEE Proc. -I*, vol. 138, pp. 169–175, June 1991.

[5] T. T. Tjhung, X. Dong, F. Adachi, and K. H. Tan, "On diversity reception of narrowband 16 star-QAM in fast Rician fading," *IEEE Trans. Veh. Technol.*, vol. 46, pp. 923–932, Nov. 1997.

[6] X. Dong, T. T. Tjhung, and F. Adachi, "Error probability analysis for 16 star-QAM in frequency-selective Rician fading with diversity reception," *IEEE Trans. Veh. Technol.*, vol. 47, pp. 924–935, Aug. 1998.

[7] V. Engels and H. Rohling, "Multilevel differential modulation technique (64-DAPSK) for multicarrier transmission systems," *Eur. Trans. Telecommun.*, vol. 6, pp. 633–640, March 1995.

[8] V. Engels and H. Rohling, "Differential modulation technique for a 34 Mbit/s radio channel using orthogonal frequency division multiplexing," *Wireless Personal Commun.*, no. 2, pp. 29–44, 1995.

[9] Y. C. Chow, A. R. Nix, and J. P. McGeehan, "Error performance of circular 16-DAPSK with postdetection diversity reception in Rayleigh fading channels," *IEE Proc. -Commun.*, vol. 144, pp. 180–190, June 1997.

[10] F. Adachi and M. Sawahashi, "Decision feedback differential detection of differentially encoded 16APSK signals," *IEEE Trans. Commun.*, vol. 44, pp. 416–418, April 1996.

[11] R. Schober, W. H. Gerstacker, and J. B. Huber, "Decision-feedback differential detection based on linear prediction for 16DAPSK signals transmitted over flat Rician fading channels," *IEEE Trans. Commun.*, vol. 49, pp. 1339–1342, Aug. 2001.

[12] Y. C. Chow, A. R. Nix, and J. P. Mcgeehan, "Analysis of 16-APSK modulation in AWGN and Rayleigh fading channels," *IEE Elec. Lett.*, vol. 28, pp. 1608–1610, Aug. 1992.

[13] M. Nakagami, "The $m$-distribution - A general formula of intensity distribution of rapid fading," in *Statistical Methods in Radio Wave Propagation* (W. G. Hoffman, ed.), pp. 3–36, Oxford: Pergamon Press, 1960.

[14] Z. Zvonar and D. Brady, "Linear multipath-decorrelating receivers for CDMA frequency-selective fading channels," *IEEE Trans. Commun.*, vol. 44, pp. 650–653, June 1996.

[15] M. K. Simon and M.-S. Alouini, *Digital Communications over Fading Channels: A Unified Approach to Performance Analysis*. John Wiley & Sons, 2000.

[16] J. G. Proakis, *Digital Communications*. McGraw-Hill, 3rd ed., 1995.

[17] P. Lombardo, G. Fedele, and M. M. Rao, "MRC performance for binary signals in Nakagami fading with general branch correlation," *IEEE Trans. Commun.*, vol. 47, pp. 44–52, Jan. 1999.

[18] Q. T. Zhang, "Exact analysis of postdetection combining for DPSK and NFSK systems over arbitrarily correlated Nakagami channels," *IEEE Trans. Commun.*, vol. 46, pp. 1459–1467, Nov. 1998.

[19] P. Y. Kam, "Bit error probabilities of MDPSK over the nonselective Rayleigh fading channel with diversity reception," *IEEE Trans. Commun.*, vol. 39, pp. 220–224, Feb. 1991.

[20] M. Abramowitz and I. A. Stegun, *Handbook of Mathematical Functions with Formulas, Graphs, and Mathematical Tables*. New York: Dover, 9th ed., 1970.

[21] M. Schwartz, W. Bennett, and S. Stein, *Communication Systems and Techniques*. McGraw Hill, 1966.

[22] A. M. Mathai and S. B. Provost, *Quadratic Forms in Random Variables: Theory and Applications*. New York 10016: Marcel Dekker, 1992.

[23] Y. Ma, C. C. Chai, and T. J. Lim, "Bit error probability for 2 and 4 DPSK in general Nakagami fading channels with correlated Gaussian noise," *IEE Proc. -Commun.*, vol. 147, pp. 155–162, June 2000.

[24] C. W. Helstrom, "Calculating error probabilities for intersymbol and cochannel interference," *IEEE Trans. Commun.*, vol. 34, pp. 430–435, May 1986.

[25] Y. Ma and Q. T. Zhang, "Accurate evaluation for MDPSK with non-coherent diversity," *IEEE Trans. Commun.*, vol. 50, pp. 1189–1200, July 2002.

[26] P. J. Lee, "Computation of the bit error rate of coherent M-ary PSK with Gray code bit mapping," *IEEE Trans. Commun.*, vol. COM-34, pp. 488–491, May 1986.

[27] X. Dong, N. C. Beaulieu, and P. H. Wittke, "Error probabilities of two-dimensional $M$-ary signaling in fading," *IEEE Trans. Commun.*, vol. 47, pp. 352–355, March 1999.

[28] R. Schober, Y. Ma, and S. Pasupathy, "On the error probability of decision-feedback differential detection," *IEEE Trans. Commun.*, pp. 535–538, April 2003.

[29] Y. Ma, T. J. Lim, and S. Pasupathy, "Error probability for coherent and differential PSK over arbitrary Rician fading channels with multiple cochannel interferers," *IEEE Trans. Commun.*, vol. 50, pp. 429–441, March 2002.

## BIOGRAPHIES

**Yao Ma** (S'98, M'01) received the B. Sc. degree from Anhui University, and M. Sc degree from University of Science and Technology of China (USTC), China, in 1993 and 1996, respectively, both in electrical engineering and information science; and the Ph.D degree in Electrical Engineering from National University of Singapore, in year 2000. His Ph.D thesis was on the diversity reception over fading channels and CDMA multiuser detection. From April 2000 to July 2001, he was a Member of Technical Staff in the Digital Communications Group at the Centre for Wireless Communications, Singapore. From July 2001 to July 2002, he was a Post-doctorate Fellow at the ECE Department of the University of Toronto. Since August 2002, he has been an Assistant Professor at the ECpE Department of the Iowa State University.

His research interests include the wireless communications over fading channels, CDMA multiuser detection, Kalman filtering, MIMO systems, and UWB communication.

**Q.T. Zhang** received the B.Eng. from Tsinghua University, Beijing, and M.Eng. from South China University of Technology, Guangzhou, China, both in wireless communications, and the Ph.D. degree in electrical engineering from McMaster University, Hamilton, Ontario, Canada. After graduation from McMaster in 1986, he held a research position and Adjunct Assistant Professorship at the same institution. In January 1992, he joined the Spar Aerospace Ltd., Satellite and Communication Systems Division, Montreal, as a Senior Member of Technical Staff. At Spar Aerospace, he participated in the development and manufacturing of the Radar Satellite (Radarsat). He was subsequently involved in the development of the advanced satellite communication systems for the next generation. He joined Ryerson Polytechnic University, Toronto in 1993 and became a Full Professor in 1999. In 1999, he took one-year sabbatical leave at the National University of Singapore, and is now with the City University of Hong Kong. His research interest is on transmission and reception over fading channels with current focus on wireless MIMO and UWB systems. He is presently an Associate Editor for the IEEE Communications Letters.

**Robert Schober** (S'98, M'01) was born in Neuendettelsau, Germany, in 1971. He received the Diplom (Univ.) and the Ph.D. degrees in electrical engineering from the University of Erlangen-Nuernberg in 1997 and 2000, respectively. From May 2001 to April 2002 he was a Postdoctoral Fellow at the University of Toronto, Canada, sponsored by the German Academic Exchange Service (DAAD). Since May 2002 he has been an Assistant Professor and Canada Research Chair (Tier II) in Wireless Communication at the University of British Columbia (UBC), Vancouver, Canada. His current research interests include noncoherent detection, ad-hoc networking, equalization, multiuser detection, MIMO systems, space-time processing and coding.

In 2001, Dr. Schober was a co-recipient of the best paper award of the German Information Technology Society (ITG). In 2002, he received the Heinz Maier-Leibnitz Award of the German Science Foundation (DFG). He also received the 2004 Innovations Award of the Vodafone Foundation for Research in Mobile Communications. Since April 2003 he has been an Editor for Detection, Equalization, and MIMO for the IEEE Transactions on Communications.

**Subbarayan Pasupathy**(F'91) was born in Chennai (Madras), Tamilnadu, India, on September 21, 1940. He received the B.E. degree in telecommunications from the University of Madras in 1963, the M.Tech. degree in electrical engineering from the Indian Institute of Technology, Madras, in 1966, and the M.Phil. and Ph.D. degree in engineering and applied science from Yale University in 1970 and 1972, respectively. He joined the faculty of the University of Toronto in 1973 and became a Professor of Electrical Engineering in 1983. He has served as the Chairman of the

Communications Group and as the Associate Chairman of the Department of Electrical Engineering at the University of Toronto. His research interests are in the areas of communication theory, digital communications, and statistical signal processing. He is a registered Professional Engineer in the province of Ontario. During 1982-1989 he was an Editor for *Data Communications and Modulation* for the IEEE Transactions on Communications. He has also served as a Technical Associate Editor for the IEEE Communications Magazine (1979-1982) and as an Associate Editor for the *Canadian Electrical Engineering Journal*(1980-1983). He wrote a regular humor column entitled "Light Traffic" for the IEEE Communications Magazine during 1984-98.

Pas S. Pasupathy was elected as a Fellow of the IEEE in 1991 "for contributions to bandwidth efficient coding and modulation schemes in digital communication", was awarded the Canadian Award in Telecommunications in 2003 by the *Canadian Society of Information Theory* and was elected as a Fellow of the *Engineering Society of Canada* in 2004.

TABLE I

GRAY-CODE BIT MAPPING FOR AMPLITUDE RATIO DETECTION AND WEIGHT FACTORS $w_a(\Delta n, \hat{\Delta} n)$ FOR DAPSK $(N, M)$ WITH $N = 4$, WHERE $\Delta\hat{\hat{n}} = (\Delta\hat{n} - \Delta n) \mod N$.

| $\Delta n$ | -3 | -2 | -1 | 0 | 1 | 2 | 3 |
|---|---|---|---|---|---|---|---|
| bit-mapping | 01 | 11 | 10 | 00 | 01 | 11 | 10 |

| $\Delta\hat{\hat{n}}$ | 0 | 1 | 2 | 3 |
|---|---|---|---|---|
| $w_a(\Delta n, \Delta\hat{n})$ | 0 | 1 | 2 | 3 |

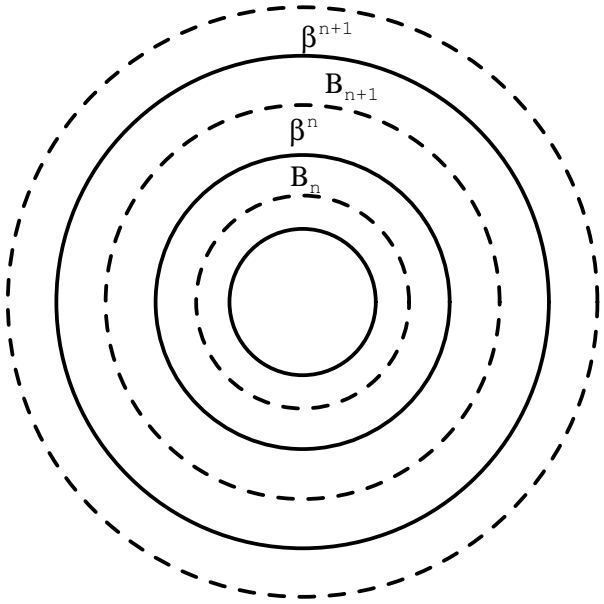


Fig. 1. The ideal amplitude ratios $\{\beta^n\}$ (rings in solid lines) and the decision boundaries $\{B_n\}$ (rings in dashed lines) for the DAPSK $(N, M)$ signal , for $n = -N + 1, \ldots, N - 1$. $B_{-N+1} = 0$ and $B_{N-1} = \infty$.

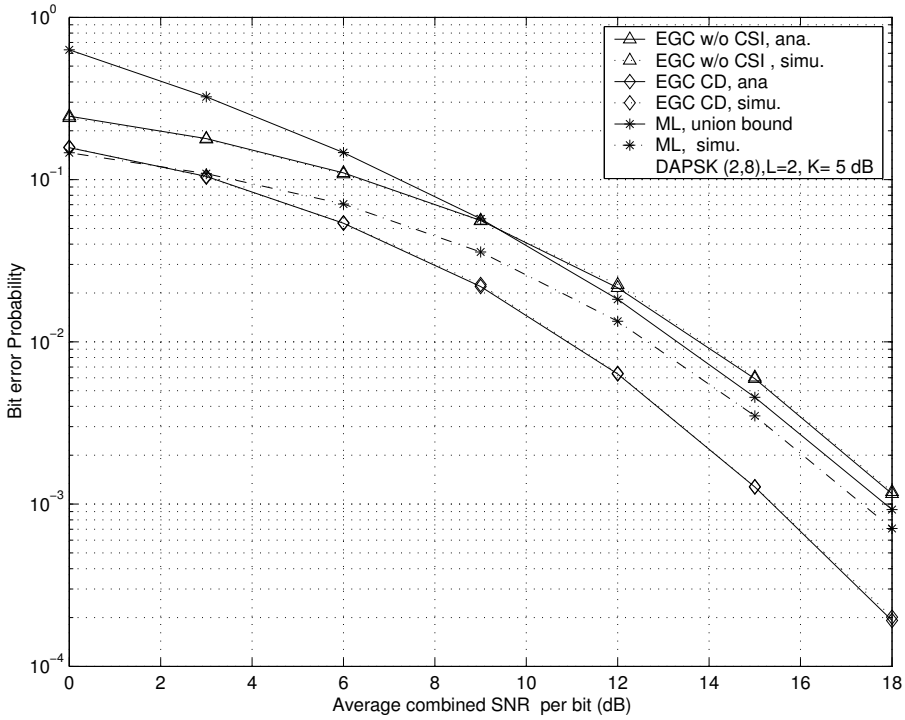


Fig. 2. BEP versus the average combined SNR per bit (in dB) for DAPSK (2,8) in an independent Rician fading channel, with $L = 2$, $K = 5$ dB, and $B_f T = 0.02$.

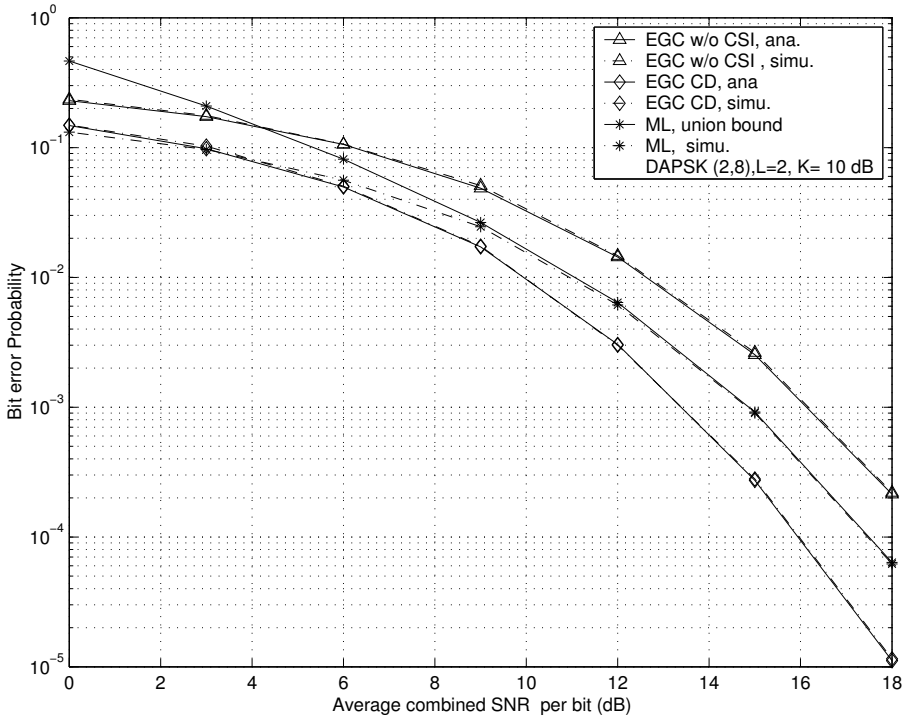


Fig. 3. BEP versus the average combined SNR per bit (in dB) for DAPSK (2,8) in an independent Rician fading channel, with $L = 2$, $K = 10$ dB, and $B_f T = 0.02$.

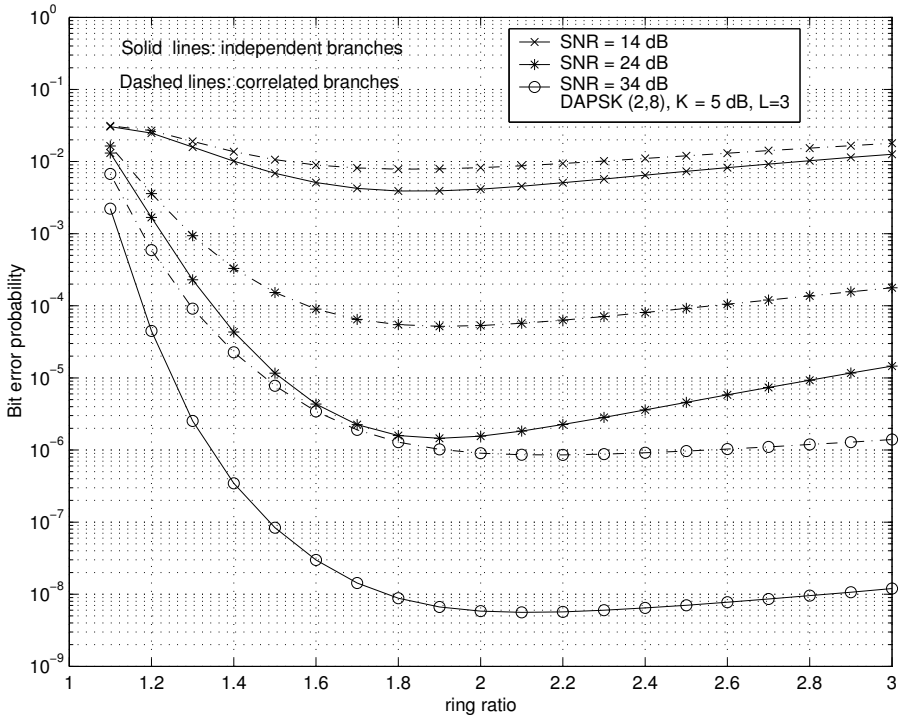


Fig. 4. BEP versus the ring ratio for DAPSK (2,8) in independent and correlated ($\rho_c = 0.5$) Rician fading channels, with $L = 3$, $K = 5$ dB, and $B_f T = 0.02$.

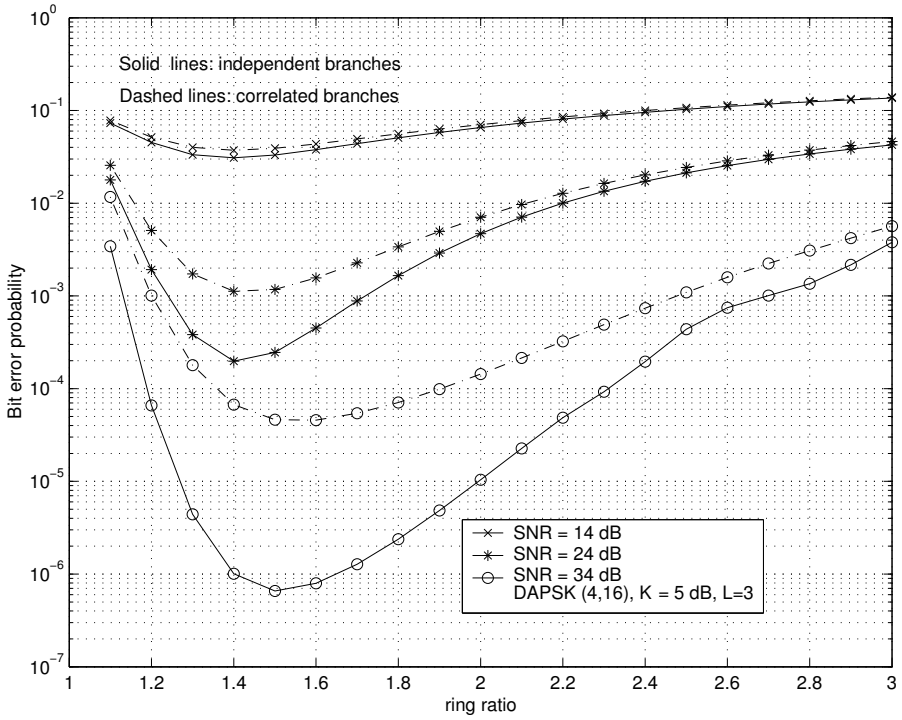


Fig. 5. BEP versus the ring ratio for DAPSK (4,16) in independent and correlated ($\rho_c = 0.5$) Rician fading channels, with $L = 3$, $K = 5$ dB, and $B_f T = 0.02$.

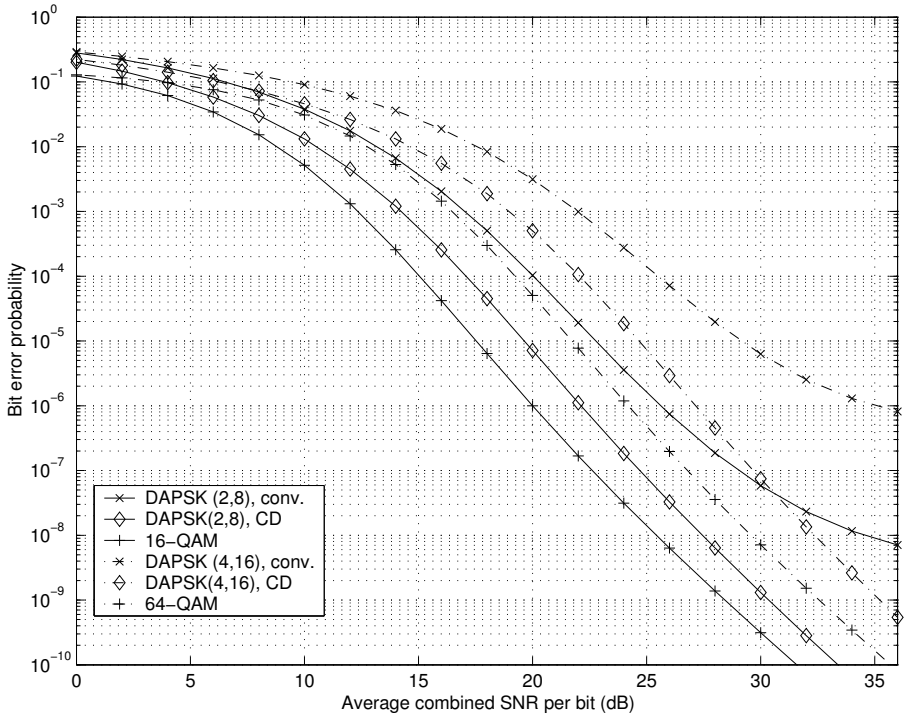


Fig. 6. BEP versus the average combined SNR per bit for DAPSK $(2, 8)$ and $(4, 16)$, and square-QAM in an independent Rician fading channel, with $L = 3$, $K = 5$ dB, and $B_f T = 0.02$.

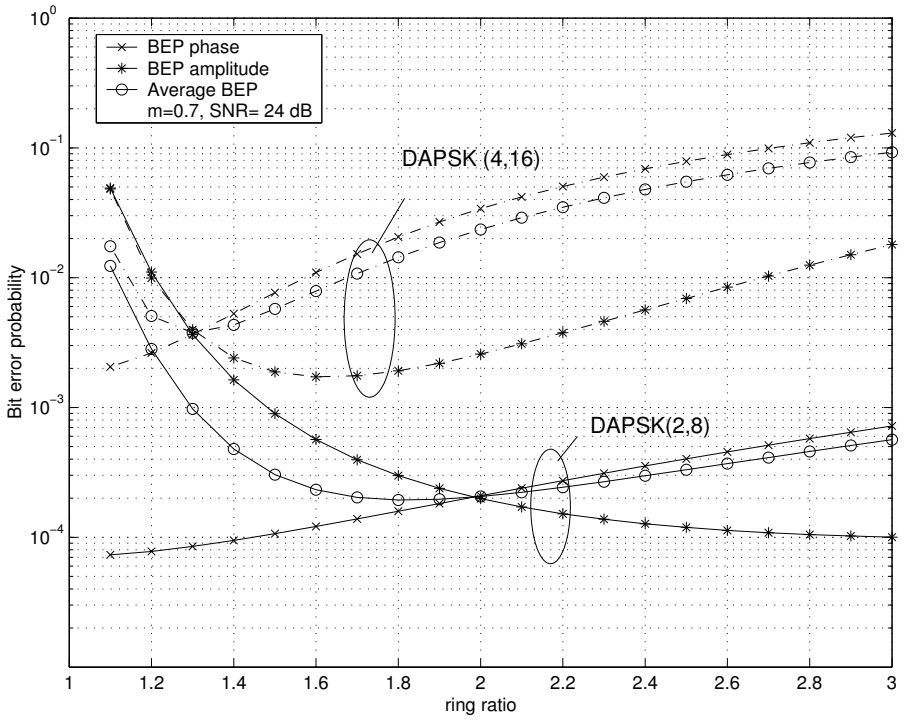


Fig. 7. Phase, amplitude, and average BEPs versus the ring ratio for DAPSK $(2, 8)$ and $(4, 16)$ in an independent Nakagami fading channel, with $L = 3$ and $m = 0.7$.

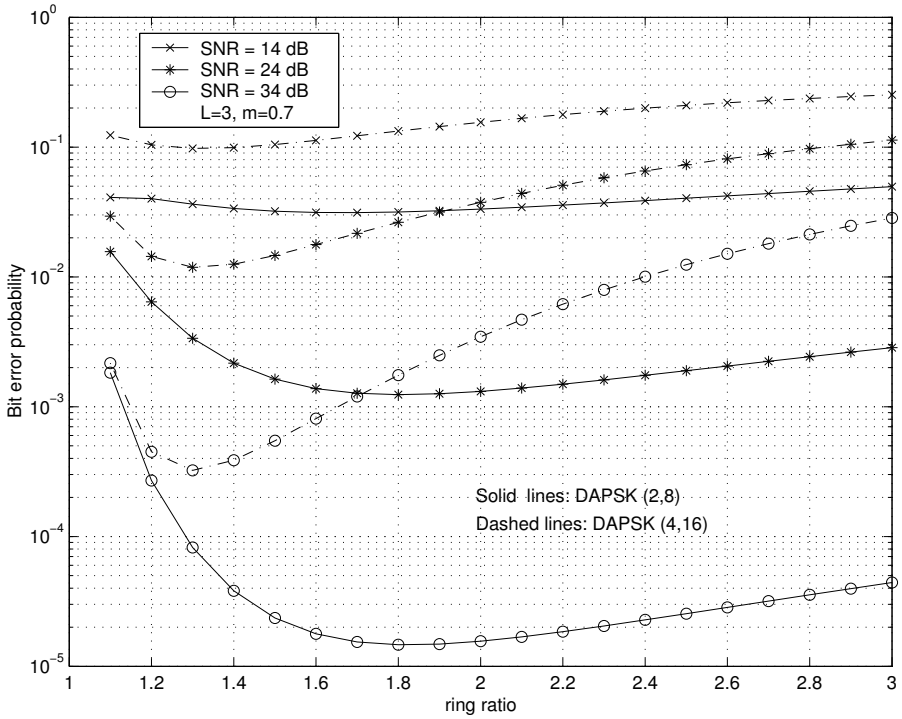


Fig. 8. BEP versus the ring ratio for DAPSK $(2, 8)$ and $(4, 16)$ in an independent Nakagami fading channel, with $L = 3$ and $m = 0.7$.

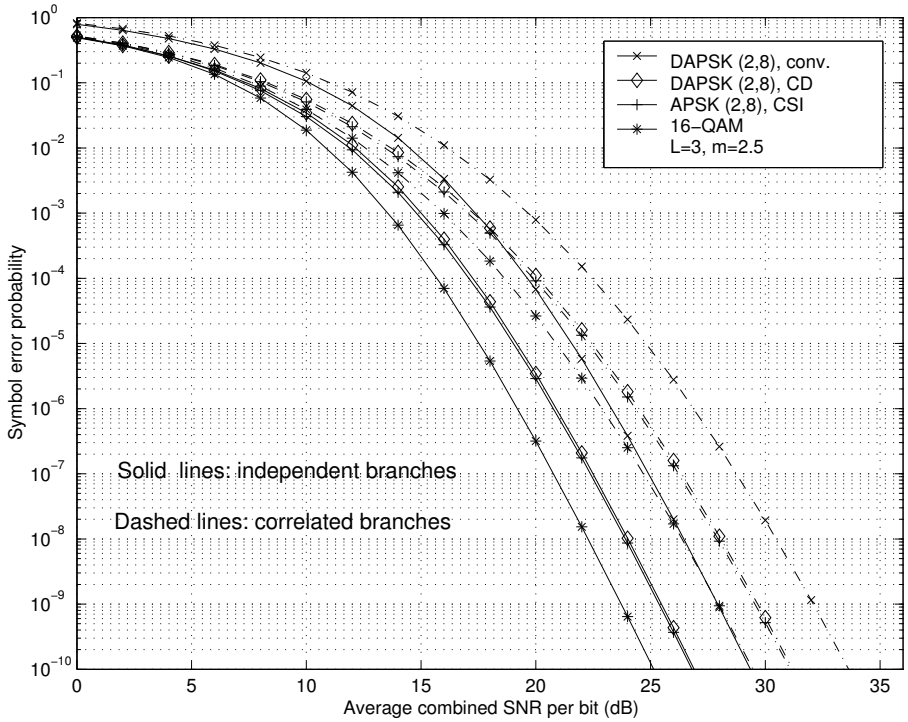


Fig. 9. SEP versus the average combined SNR per bit for DAPSK $(2, 8)$, APSK (2,8) (all with $\beta = 2$), and 16-QAM in independent and correlated Nakagami fading channels, respectively, with $L = 3$ and $m = 2.5$.